# ADVANCED OPTICAL MATERIALS



FRET
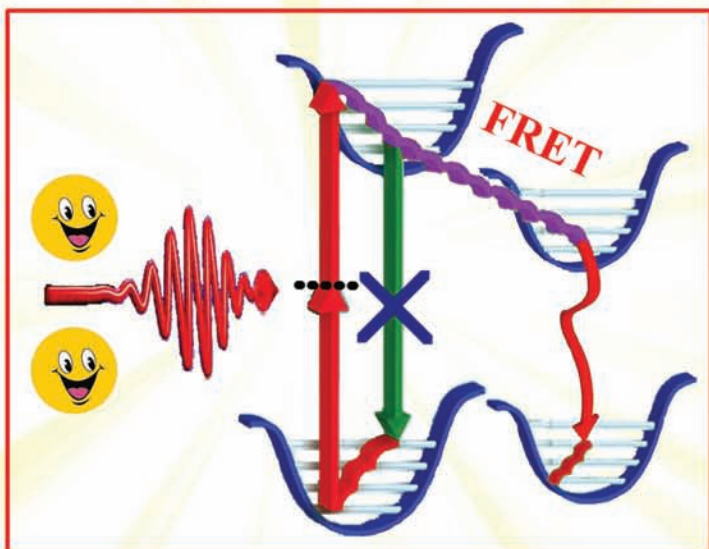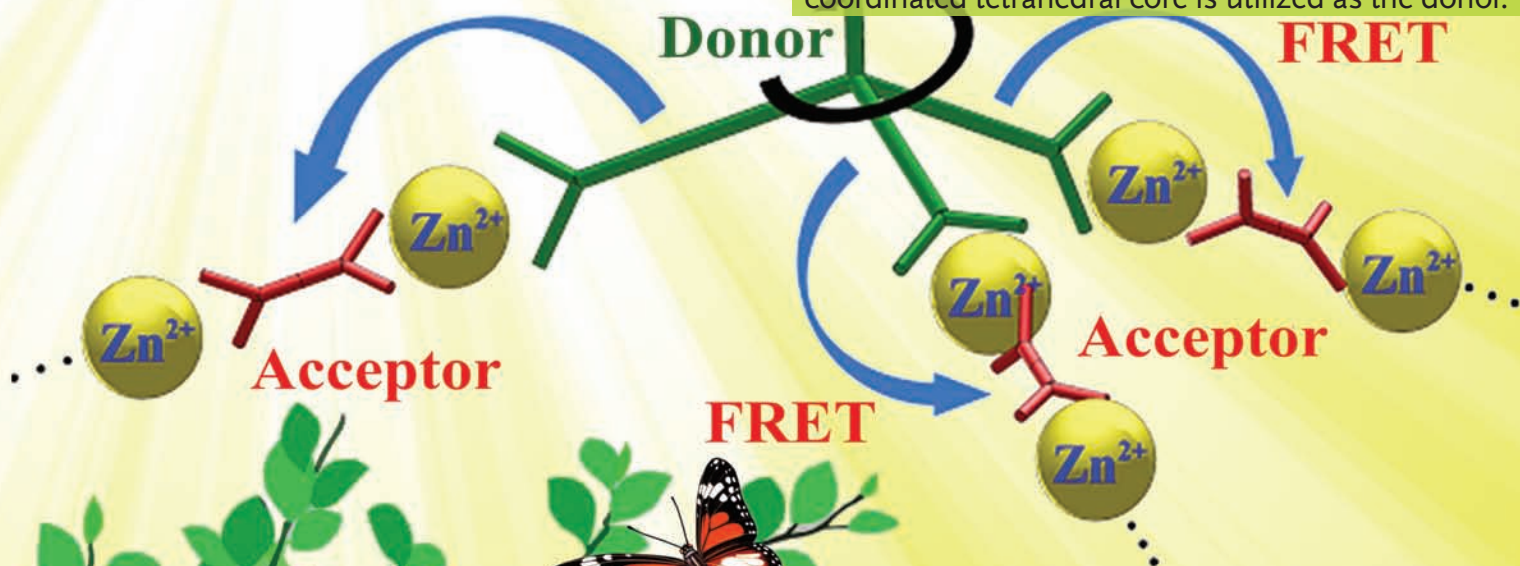
Acceptor

FRET

**NONLINEAR OPTICS**

H. Sun and co-workers demonstrate a novel 3D two-photon-type light-harvesting system which may be directly used for in vivo bioimaging and nonlinear optical devices. As shown on page 40, two-photon excited Förster resonance energy transfer (FRET) is exploited to enhance the solid-state fluorescence of a supramolecular centre (acceptor) in an artificial 3D metal-organic complex (MLC), in which a 3D Zn(II)-coordinated tetrahedral core is utilized as the donor.

FRET

Donor

$Zn^{2+}$

$Zn^{2+}$

$Zn^{2+}$

$Zn^{2+}$

$Zn^{2+}$

Acceptor

Acceptor

FRET

**ADVANCED
OPTICAL
MATERIALS**

www.advopticalmat.de

**Materials Views**

www.MaterialsViews.com

# Efficient Energy Transfer under Two-Photon Excitation in a 3D, Supramolecular, Zn(II)-Coordinated, Self-Assembled Organic Network

*Tingchao He, Rui Chen, Zheng Bang Lim, Deepa Rajwar, Lin Ma, Yue Wang, Yuan Gao, Andrew C. Grimsdale, and Handong Sun\**

Multiphoton excited fluorescence of organic molecules is promising in the applications of efficient nonlinear optical devices and bioimaging. However, they usually have disadvantages of poor photostability and serious fluorescence quenching in aqueous media or solid state, which seriously limit their related applications. In this work, for the first time, the two-photon excited Förster resonance energy transfer (FRET) process is used to enhance the solid-state fluorescence of the supramolecular centre (acceptor) in an artificial 3D metal–organic complex (MLC), in which a 3D Zn (II)-coordinated tetrahedral core is utilized as the donor. More interestingly, the two-photon light harvesting system, which can be pumped with an optical intensity as low as 1 MW/cm$^2$, exhibits an ultrafast energy transfer rate (∼6.9 × 10$^8$ s$^{-1}$) and ultrahigh photostability. The underlying physical mechanisms are revealed through comprehensive steady-state and time-resolved spectroscopic analysis. This work demonstrates that the 3D MLC can be directly used in two-photon bioimaging and also sheds light on developing other multiphoton harvesting systems, such as metal–organic frameworks.

## 1. Introduction

Organic chromophores or crystals with large two-photon absorption (TPA) in the solid state are very much demanded for applications in optical limiting, frequency-upconversion lasing, laser pulse stabilization and reshaping etc.[1,2] In particular, efficient two-photon excited fluorescence emission or absorption that can be achieved at low optical intensity with the near infrared wavelengths is very important in practical nonlinear optical devices or biomedical imaging.[3,4] To obtain large TPA cross-sections, various molecular structures have been designed. Unfortunately, these strategies are usually only valid in organic solvents.[5] They suffer from poor photostability and serious fluorescence quenching in aqueous media or solid state due to aggregation to different extents,[6] which is especially unfavourable for the applications in biological imaging and solid state devices.[7] Therefore, developing organic chromophores with strong two-photon excited fluorescence and high photostability in the solid state remains challenging for various practical applications.[8]

Besides the design of organic systems at the molecular level to achieve large two-photon absorbing dyes, an alternative method is to make use of two-photon excited Förster resonance energy transfer (FRET). In this case, the donors are used as two-photon light-harvesting antenna to capture energy, and then the electronic excitation is subsequently transferred to a suitable acceptor.[9] As is well-known, in order to obtain efficient one-photon excited FRET, the following aspects must be satisfied: 1) the donor has a high quantum yield; 2) substantial overlap of the donor's emission with the acceptor's absorption; 3) close distance between donor and acceptor which is beneficial for the occurrence of nonradiative dipole–dipole coupling.[10] Furthermore, the excited state lifetime of the donor must be long enough to allow the energy transfer to occur and to compete with other deactivation processes. In addition to the basic requirements aforementioned, to make two-photon excited FRET more generally applicable, the design of organic molecules with large TPA cross-section is required, which makes sure the two-photon absorbing materials to act as efficient donors to transfer the harvested energy to the acceptor.[11] The acceptors are thus indirectly excited through the transfer of two-photon excited energy, resulting in the significant enhancement of two-photon excited fluorescence efficiency. Although many efforts has been made to study one-photon excited FRET process, two-photon excited FRET has been studied rarely in solution, and has never been studied in the solid state. This is because the design and synthesis of

Dr. T. He, Dr. R. Chen, L. Ma, Y. Wang,
Y. Gao, Prof. H. Sun
Division of Physics and Applied Physics
School of Physical and Mathematical Sciences
Nanyang Technological University
Singapore 637371, Singapore
E-mail: hdsun@ntu.edu.sg
Prof. H. Sun
Centre for Disruptive Photonic Technologies (CDPT)
Nanyang Technological University
Singapore 637371, Singapore
Dr. Z. B. Lim, D. Rajwar, Prof. A. C. Grimsdale
Division of Materials Technology
School of Materials Science and Engineering
Nanyang Technological University
Singapore 639798, Singapore

www.MaterialsViews.com

ADVANCED
OPTICAL
MATERIALS
www.advopticalmat.de

FULL PAPER

large two-photon absorbing dyes, which will not cause a red-shift of the emission wavelength and decreases the fluorescence quantum yield and photostability, still represents a significant challenge.

Metal-ligand complexes (MLC), made from organic linkers and inorganic nodes, have found wide applications in gas storage, sensing, chemical delivery and nonlinear optics, thanks to their excellent chemical and physical properties.[12] The ability to conveniently tune the molecular building blocks in MLCs makes them ideal model systems for studying energy transfer in ordered solid state.[13–15] If two-photon absorbing dyes are used as donors in the MLCs, efficient energy transfer and enhanced photostability properties can be synergized, and novel MLCs working at low excitation intensity and with high photostability where the two-photon excitation energy can be efficiently harvested by acceptors should be possible. However, to date, two-photon induced FRET in MLCs has never been demonstrated.

Our previous work demonstrated that terpyridine-based Zn(II)-coordinated rigid linear polymers exhibited large wavelength dependent optical nonlinearities in organic solvents.[16] However, such kinds of metallopolymers had poor two-photon excited fluorescence emission properties and photostability

in solid state films, preventing them from practical applications in nonlinear optical devices. Herein, we utilize a newly synthesized tetrahedral molecule to build up an excellent multiphoton-absorbing chromorphore, which exhibits fluorescence efficiently by absorbing even five photons. By Zn(II)-coordination of this tetrahedral core, the 3D MLC is constructed as a multiphoton absorbing donor (3D light-harvesting antenna) to transfer the absorbed energy to the acceptor in an extended 3D MLC. As a result, in the extended 3D MLC, not only the multiphoton excited fluorescence from acceptor has been greatly increased, but also the photostability has been significantly improved.

## 2. Results and Discussions

**Figure 1** depicts the design of the Zn(II)-coordinated self-assembled extended 3D MLC. Briefly, the tetrahedral core (Figure 1a) was synthesized and then refluxed with 2 equivalents of Zinc acetate in NMP solution followed by anion exchange using an excess of $NH_4PF_6$ to obtain the tetraphenylmethane-based 3D MLC, depicted in Figure 1b, which was used as two-photon absorbing donor. This donor cannot be dissolved in common
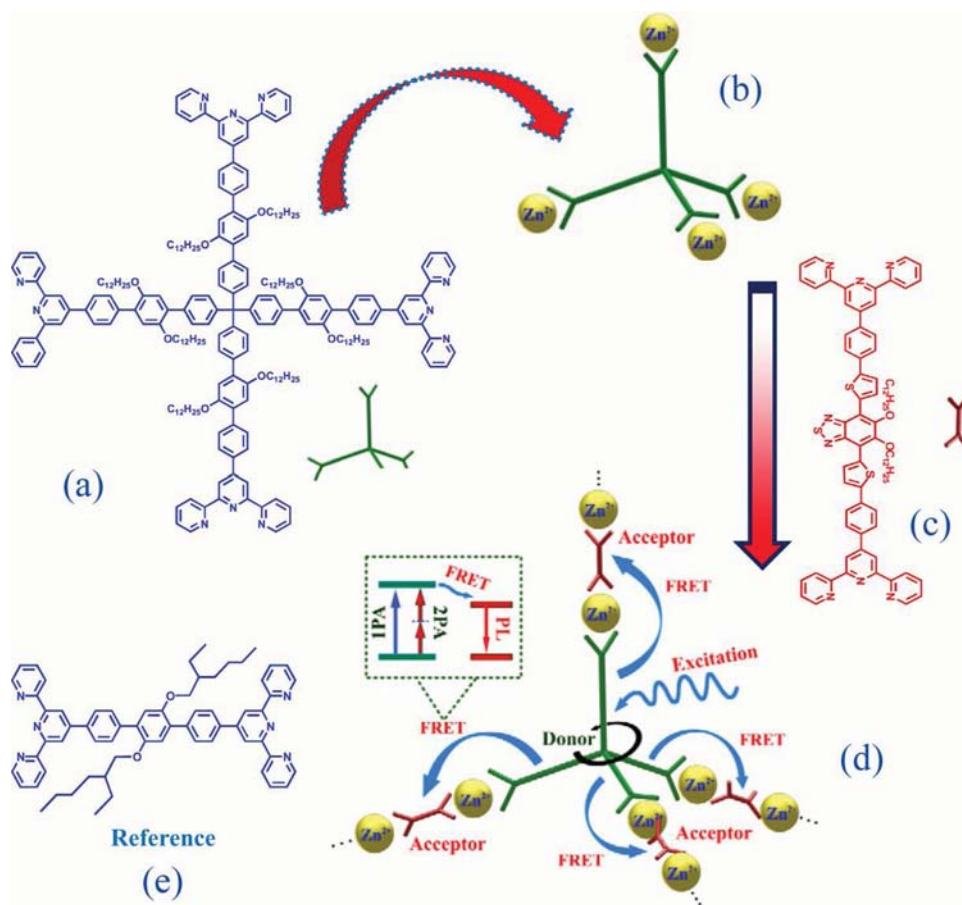


**Figure 1.** Schematic diagram of the synthesis of extended 3D MLC. a) Tetrahedral molecule used for the construction of donor; b) Tetraphenylmethane-based 3D MLC used as two-photon absorbing donor; c) Uncoordinated monomer and more Zn ions used to construct the acceptor in the extended 3D MLC; d) The photoinduced energy transfer process in the extended 3D MLC under the excitation of one- and two-photon. e) Linear chromophore used for reference sample.

solvents due to its highly crosslinked or interpenetrated structure. Finally, due to the reversible nature of the 3D coordinated network, addition of 2 equivalents of zinc and 2 equivalents of the linear bisterpyridyl linker unit (uncoordinated acceptor, Figure 1c), followed by anion exchange with $NH_4PF_6$, could produce the extended 3D MLC (Figure 1d). This expanded 3D MLC was more porous than the donor, but the porosity and surface area were still lower compared to common metal-organic frameworks (MOFs), suggesting a high degree of interpenetration remained within the expanded network. The detailed synthesis and characterization of the above materials can be seen elsewhere.[17]

In order to provide important information for the analysis of the two-photon excited energy transfer process in the extended 3D MLC, we examined the linear and nonlinear optical properties of the tetrahedral core that was used to construct the donor. For comparison, the optical properties of a bisterpyridyl monomer with similar structure, as shown in Figure 1e, was also investigated. **Figure 2**a and b show the UV-vis linear absorption and emission spectra of the two chromophores in THF

solutions with a concentration of $1 \times 10^{-5}$ M. Both of the molecules showed similar broad and structured absorption bands and strong blue emission peaking at around 441 nm. Using quinine sulfate monohydrate in 0.1 M $H_2SO_4$ ($\Phi = 0.58$) as a standard, the quantum yields for both of the linear and tetrahedral molecules were determined to be 11% in THF solutions. Moreover, from the inset of Figure 2b, the lifetime of tetrahedral molecule ($\tau = 1.3$ ns) was increased compared to that of its linear counterpart ($\tau = 1.0$ ns), which was advantageous for energy transfer. The increased lifetime of tetrahedral molecule should be attributed to the increased molecular steric effect, which restricted its free mobility and inhibited the nonradiative decay of fluorescence. To elucidate the influence of the molecular structure on the nonlinear optical properties, the multiphoton excited fluorescence emission properties were investigated by using femtosecond pulses as excitation source. Interestingly, tetrahedral molecule even showed strong fluorescence under two- to five-photon excitation. The multiphoton excited fluorescence spectra were very similar to those of one-photon excitation, thereby suggesting that their fluorescence emission states should be the same. Figure 2c shows the comparison of two-photon excited fluorescence spectra (excited at 720 nm) of linear and tetrahedral molecules. Inset is the emission intensity versus the square of the excitation power. The log–log plots with slope values of around 2 indicate that the optical process is of TPA nature.[5] Another advantage of the tetrahedral molecule was its high solubility (up to 30 mg/mL), which was among the most soluble dyes and allowed it to be easily fabricated. The TPA spectra of two chromophores, measured by using the Z-scan technique,[18,19] are presented in Figure 2d. Remarkably, the maximum TPA cross-section ($\sigma_{max} = 2368$ GM) of the tetrahedral core was found to be 7 times greater than that of its linear counterpart ($\sigma_{max} = 383$ GM) between 710 and 825 nm, highlighting the synergetic effect of the tetrahedral structure for TPA enhancement. Such an enhancement was attributed to dipole–dipole-type or $\pi$-conjugation-type interactions between the tetrahedral molecule's branches, which resulted in the formation of coupled excited states favorable for TPA.[20] Though tetrahedral molecule exhibited moderate TPA cross-section compared to some reported organic molecules with red emission, it was among the maximum values for blue emission molecules.[5,21] Moreover, two-photon excited light harvesting through FRET was a synergic effect of many factors. Large two-photon absorbing molecules did not mean that they would be good donors for FRET under TPA. One must consider their photostability, spectral overlap with acceptor and lifetime. As a matter of fact, in many cases, despite the good spectral overlap between
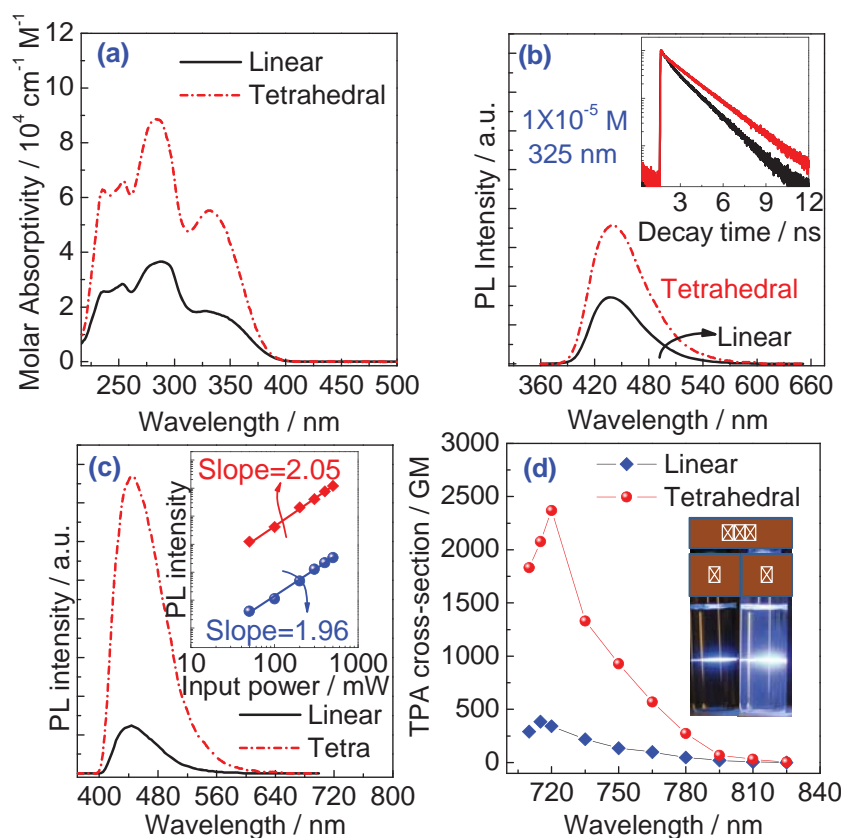


**Figure 2.** a) UV-vis absorption spectra and b) Fluorescence emission spectra of linear and tetrahedral chromophores dissolved in THF solutions with a concentration of $1 \times 10^{-5}$ M. The inset in Figure 2b shows their fluorescence decay curves, detected at 441 nm; c) Two-photon excited fluorescence spectra of the chromophores in THF solutions at 720 nm. Inset is the emission intensity versus the excitation power intensity. The log–log plots with slope values of around 2 indicate the nature of TPA; d) TPA spectra of two chromophores in THF solutions with a concentration of $1 \times 10^{-4}$ M. The inset shows the images of two-photon excited fluorescence for linear (1) and tetrahedral (2) chromophores at an excitation intensity of 1 GW/cm², under the excitation wavelength of 720 nm.

www.MaterialsViews.com

ADVANCED
OPTICAL
MATERIALS
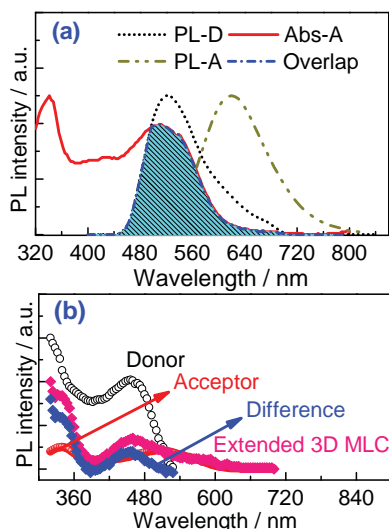www.advopticalmat.de

FULL PAPER

**Figure 3.** a) Absorption and emission spectra of the components in solid state: PL-D represents emission spectrum of donor, and PL-A and Abs-A represent the emission and absorption spectra of Zn-coordinated homopolymer (acceptor), respectively. The spectra are scaled to the same height at their respective maxima. The spectral overlap is highlighted in blue color; b) Excitation spectra of donor detected at 525 nm, acceptor detected at 625 nm and the extended 3D MLC detected at 625 nm. The blue open squares represent the fraction of energy transfer from the donor to acceptor, which resembles the excitation spectrum of donor.



**Figure 4.** a) Fluorescence decay curves of the donor and extended 3D MLC, detected at 525 nm; b) Fluorescence decay curves of acceptor and extended 3D MLC under the excitation of 360 nm, detected at 625 nm.

donor and acceptor, inefficient FRET from donor to acceptor was observed due to the unfavorable orientation between their transition dipole moments.[22] Interestingly, the tetrahedral structure motif can also give rise to a large enhancement of three- to five-photon absorption properties relative to linear counterpart without causing a red-shift of the emission spectrum and decrease of quantum yield (Figures S1–S3, Supporting Information). Therefore, it was possible to use the tetraphenylmethane-based 3D MLC as a donor to develop highly effective multiphoton excited FRET if a suitable acceptor was adopted.

To facilitate the investigation of the nonlinear optical property of 3D MLCs, we started the experiments by using continuous-wave UV excitation. From these experiments, we could achieve a lot of important information, such as the electronic structures of molecules, which was indispensable to analyze the related physical mechanisms under two-photon excitation.[9a,11] **Figure 3**a shows the spectra of emission and absorption for donor and acceptor. Obviously, there was a favorable overlap between the emission of donor and the absorption of acceptor. Such large spectral overlap was important to satisfy the basic requirements for efficient energy transfer.[23] Under the excitation of 360 nm, although the individual donor alone exhibited strong emission, the donor emission was almost completely quenched and only the emission from the acceptor was observed in the extended 3D MLC. Moreover, only acceptor emission appeared in the extended 3D MLC under the excitation of 325–570 nm (Figure S4, Supporting Information), directly indicating the broadband energy transfer in the extended 3D MLC. The energy transfer process can be realized by either FRET or reabsorption, which can be distinguished by
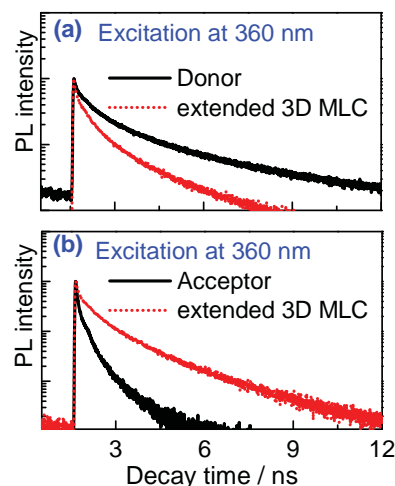
measuring the excitation spectra and time-resolved photoluminescence (TRPL) spectra.[24,25] As a result of energy transfer, the contribution of donor to acceptor emission can be estimated by comparing the excitation spectra of acceptors alone and in extended 3D MLC.[24] As shown in Figure 3b, compared to the excitation spectra of acceptor, there was a distinct additional component in a region corresponding to the absorption of donor. By calculating the difference of extended 3D MLC relative to pure acceptor recorded at 625 nm, we can estimate the contribution of donor to acceptor emission in the extended 3D MLC through energy transfer. The difference plotted versus the wavelength resembled the excitation spectrum of donor, stressing the fact of FRET.

To gain further insight into the energy transfer process, TRPL measurements monitoring the donor emission at 525 nm were performed and the results are depicted in **Figure 4**a. The emission lifetimes were obtained from time-correlated single photon counting (TCSPC) technique, and we were also able to calculate the FRET parameters describing the energy transfer dynamics. The energy transfer efficiency as calculated from the measurements is given by the Equation (1)

$$E = 1 - \frac{\tau}{\tau_0} \tag{1}$$

where $\tau$ is the fluorescence lifetime of the donor in the presence of the acceptor and $\tau_0$ is the fluorescence lifetime of the donor in the absence of the acceptor.[26] Their average lifetimes were determined to be 0.59 and 1.0 ns, as presented in Figure 4a, respectively. Figure 4b depicts the fluorescence decay curves detected at 625 nm from the acceptor in absence of donor and the extended 3D MLC. Under the excitation of 360 nm, the emission at 625 nm from the extended 3D MLC became slower due to the delayed excitation provided by the donor through FRET compared to the pure acceptor. As a result, the lifetime of acceptor increased from 0.13 to 0.56 ns in the extended 3D MLC. The shortened lifetime of donor accompanied by the increase of acceptor lifetime in principle was due to FRET, because FRET acted as an extra energy-decay channel.[27–29,30a]

ADVANCED
OPTICAL
MATERIALS
www.advopticalmat.de

Materials
Views
www.MaterialsViews.com

The energy transfer efficiency as calculated from the TRPL measurements was 41% in the extended 3D MLC.

As the difference of excitation spectra of the acceptors in the extended 3D MLC and in absence of donor followed the trend of donor excitation spectrum (Figure 3b), strongly indicating the shortening of donor lifetime in the extended 3D MLC was due to FRET, rather than the aggregation induced quenching effect in solid state. Meanwhile, the energy transfer rate ($k_{ET}$) and energy tranfer time ($1/k_{ET}$) can be determined from the quenched and unquenched excited-state lifetimes of the donor using Equation (2):[26]

$$k_{ET} = \frac{1}{\tau} - \frac{1}{\tau_0} \qquad (2)$$

Apparently, the energy transfer rate and energy tranfer time can be determined by $6.9 \times 10^8$ $s^{-1}$ and 1.44 ns, respectively. Though the energy transfer rate here was smaller compared to that of semiconductor quantum dots and a redox-active osmium assembly,[31] it was comparable to that of porphyrin-based MOFs with CdSe/ZnS core/shell quantum dots and hybrid conjugated polymer/quantum dot nanocomposites,[30] and even faster mesoporous SBA-15 silica system and CdSe/ZnS core/ shell quantum dot-dye-loaded zeolite L nanoassemblies.[26,32]

It was worthwhile to note that the decrease of blue emission of tetrahedral core was accompanied by a reduction in the emission from uncoordinated acceptor when the two compounds were physically mixed in THF directly (Figure S5, Supporting Information), which was indicative of efficient interaction but an absence of FRET between them. Hence, the coordination of tetrahedral core and uncomplexed acceptor was essential for the generation of FRET in the extended 3D MLC.

It is well known that the molecules would suffer from aggregation induced fluorescence quenching or enhancement in solid state.[33] To better understand the mechanism of two-photon excited energy transfer process, we needed to compare the quantum yields of materials in organic solvents and solid state. Since the donor cannot be dissolved into organic solvents, only its quantum yields in the solid state were measured. As was expected, the quantum yield of the donor decreased from 9% in absence of acceptor to 4% in the extended 3D MLC due to the additional nonradiative decay channel (FRET). For the acceptor, its quantum yield changed from 7% in DMSO to 6% in solid state. Meanwhile, its quantum yield remained constant (6%) when the donor was added in 3D MLC. As the FRET mechanism was confirmed by one-photon steady-state and time-resolved spectroscopic measurements, two-photon excited FRET also could be expected due to the large TPA properties of donor, even though their application sceneries were different. In the case of one-photon excitation, the energy transfer was induced due to the enhancement of linear absorption in the extended 3D MLC. While under two-photon excitation, the donor transferred the two-photon absorbing energy to the acceptor, and the magnitude of population generated in the excited state of acceptor can be as large as direct single-photon pumping. Obviously, although not a determinant factor, the donor with large TPA was vital, which acted as two-photon light harvester to enhance the emission from the acceptor. Therefore, we needed first to investigate the TPA properties of the donor. Under excitation at 720 nm, the donor presented strong two-photon excited fluo-
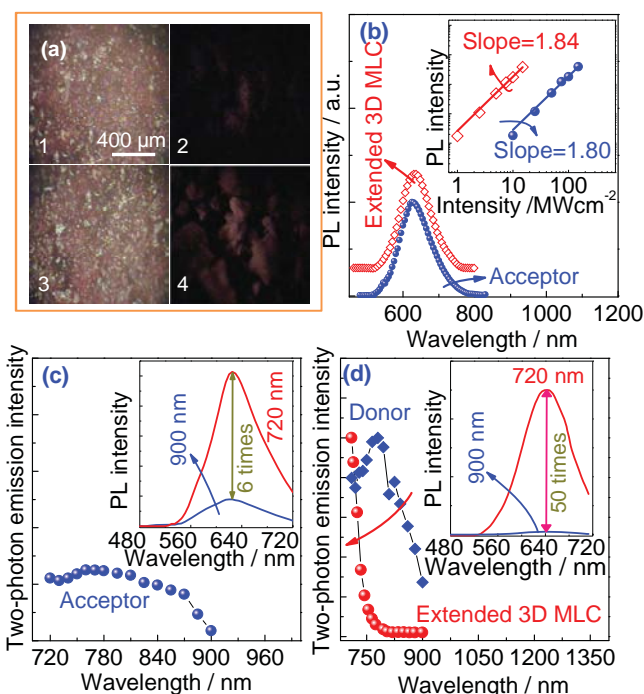


**Figure 5.** a) Images of the appearance for acceptor (1) and extended 3D MLC (3). Two-photon excited fluorescence images for acceptor (2) and extended 3D MLC (4) at the wavelength of 720 nm with excitation intensity of $1 \times 10^7$ W/cm$^2$. The inset in (1) is the scale bar; b) Square dependence of two-photon excited fluorescence intensity on the excitation intensity at 720 nm, for both acceptor and extended 3D MLC, confirming the process of TPA; Two-photon excited fluorescence intensity versus excitation wavelength range from 720 to 900 nm for c) acceptor and d) extended 3D MLC. The insets depict the comparison of emission spectra at 720 and 900 nm.

rescence while its shape was almost the same with that from one-photon excitation (Figure S6, Supporting Information), indicating that in both excitation processes the fluorescence emissions originated from the same excited state. Images of the appearance and fluorescence emission (excited at 720 nm with an optical intensity of $1 \times 10^7$ W/cm$^2$) of pure acceptor and extended 3D MLC are also shown in **Figure 5**a. A low-pass filter (<720 nm) was used to block excitation light when capturing the images of fluorescence emission. Apparently, the extended 3D MLC exhibited brighter red fluorescence compared to pure acceptor, further indicating that energy transfer related emission enhancement occurred. As shown in Figure 5b, though the donor displayed strong two-photon excited fluorescence emission, it was also completely quenched in the extended 3D MLC and the emission envelope of extended 3D MLC was very similar to that from pure acceptor. To verify that the observed fluorescence was induced by two-photon excitation, the dependence of emission intensity on excitation power intensity was measured. As shown in the inset of Figure 5b, the two-photon excited fluorescence intensity was proportional to the square of the excitation intensity, confirming the characterization of two-photon process. Despite the FRET efficiency of the 3D MLC was moderate compared to some one-photon light harvesting systems in organic solutions,[34] this was the first attempt to

achieve two-photon excited light harvesting system in solid state. We also needed to note that previous experiments were always carried out in solutions, they would usually suffer from quenching (or decrease of energy transfer efficiency) to different extent. Again, two-photon excited fluorescence intensity at different wavelengths was measured for the acceptor, donor and extended 3D MLC, which can provide the energy transfer related information due to the selective excitation of donor and acceptor. Figure 5c shows the two-photon excited fluorescence intensity of acceptor under different excitation wavelength. As indicated in the inset of Figure 5c, the two-photon excited fluorescence intensity increased by 6 times with the excitation wavelength shifting from 900 to 720 nm due to near resonance effect.[35] By contrast, in the extended 3D MLC, the ratio of two-photon excited fluorescence intensity at 720 nm to that at 900 nm was up to 50 times, as shown in the inset of Figure 5d. Hence, the enhancement factor of acceptor emission intensity was up to 8.3 times. Consistent with the large enhancement factor, two-photon excitation spectrum of donor peaked at 780 nm as depicted in Figure 5d, much far from the wavelength of 900 nm. Influenced by the energy transfer from the donor, the peak of two-photon spectrum from extended 3D MLC further shifted towards shorter wavelength.

The large enhancement factor, obtained under two-photon excitation, implied the big difference between TPA cross-sections of donor and acceptor. With large TPA in donors, the energy harvested from excitation source in extended 3D MLC was more efficient than the direct excitation of acceptor. As a result, not only was a large enhancement factor obtained, but also a low excitation intensity could be used to achieve two-photon excited fluorescence from extended 3D MLC. Interestingly, even under an unfocussed laser beam with the optical intensity as low as $1 \times 10^6$ W/cm$^2$, strong two-photon excited fluorescence from the extended 3D MLC could still be observed. Although the excitation intensity was higher than those used for some two-step upconversion materials ($\leq 1 \times 10^4$ W/cm$^2$), such as rare-earth-doped dielectrics[36] and recently reported colloidal double quantum dots,[37] which was three orders of magnitude lower than those required for simultaneous TPA (typically ~1 GW/cm$^2$), highlighting the potential of practical applications in solid state nonlinear optical devices. Moreover, the quantum yield of our two-photon harvesting systems (6%) was much higher than those of two-step upconversion materials (<2%). The advantageous properties of the extended 3D MLC should be attributed to our dedicated design incorporating an efficient two-photon absorbing donor.

For the practical application in solid state nonlinear optical devices, the materials must demonstrate good photostability under laser operation.[38] Usually, there is a tradeoff between fluorescence enhancement factor and photobleaching time of samples. To further investigate the photostability of extended 3D MLC, bleaching tests were carried out on the close-packed solid films of the acceptor and extended 3D MLC. As shown in **Figure 6**a, the emission intensity of acceptor was found to undergo a dramatic decrease by 90% when the samples were continually exposed to the UV laser excitation of 325 nm with a power intensity of 1 W/cm$^2$, while the emission intensity of extended 3D MLC under the same conditions remained unchanged for 2000 s. Similarly, under the excitation of
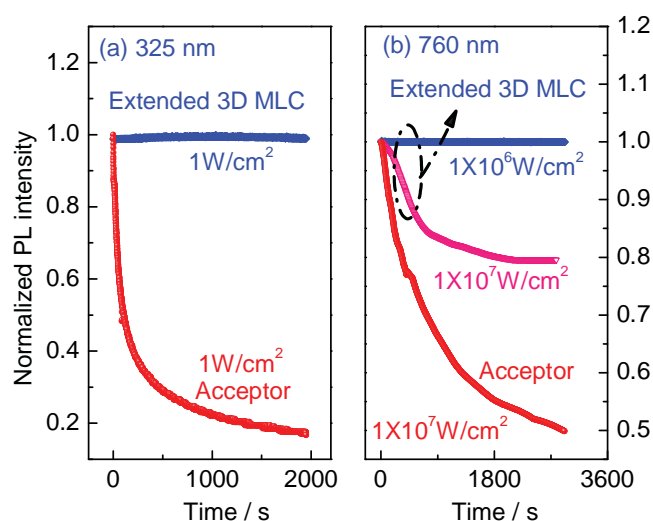


**Figure 6.** Normalized emission intensity as a function of time for acceptor and extended 3D MLC with detection at 625 nm a) under the excitation of 325 nm and b) under the excitation of 760 nm.

760 nm with an optical intensity of $1 \times 10^7$ W/cm$^2$, the extended 3D MLC suffered from 20% emission decrease while the decrease could be up to 50% for acceptor in absence of donor. More interestingly, at the optical intensity of $1 \times 10^6$ W/cm$^2$, which could efficiently pump the extended 3D MLC but was not able to excite the pure acceptor in absence of donor, the two-photon excited fluorescence from extended 3D MLC exhibited excellent photostability, maintaining 100% of its initial emission after 2800 s. Due to larger molecular size for the extended 3D MLC (or lower molecular density), the average excitation intensity irradiated on each molecule would become even larger. Therefore, the acceptor in the extended 3D MLC undoubtedly exhibited increased photostability compared to acceptor in absence of donor. Its enhanced photostability should be related to the excellent thermal resistance induced by the FRET process, where the donor would disperse the partial absorbed energy. Moreover, the quantum yields of acceptor in the extended 3D MLC remained constant in the whole absorption band compared to the acceptor in absence of donor, indicating there was no ground state interaction between donor and acceptor. Additionally, the acceptor was also a Zn-coordinated metallopolymer. Therefore, the increased photostability of the acceptor in the extended 3D MLC was due to FRET, rather than metal coordination. Clearly, the excitation of donor and following FRET process significantly enhanced the photostability of extended 3D MLC under consideration, demonstrating that constructing 3D MLC was a promising technique to improve photostability of two-photon excited fluorescence emission. For comparison purpose, we have also given the relative emission intensities of the samples at different pumping intensity (Supporting Information, Figure S7). Again, we needed to point out that we did not intend to compare the differences in the physical processes under one- and two-photon excitation. The photostability test experiments presented here using 325 nm excitation were utilized to further confirm that the same conclusions can be achieved under

one- and two-photon excitation, as FRET process would boost the photostability in both cases.

## 3. Conclusion

By using tetraphenylmethane-based 3D MLC as a two-photon absorbing donor, we have demonstrated efficient energy transfer, enhanced two-photon property and improved photostability of the solid state extended 3D MLC. Comprehensive steady-state and time-resolved spectroscopic measurements are employed to validate FRET occurring through electronic transition dipole interactions. This is the first time that the two-photon excited FRET process has been investigated in artificial 3D MLCs. The novel 3D two-photon type light-harvesting system can be directly used for in vivo bioimaging and non-linear optical devices. Further studies along the work may help to advance the design of other two-photon excited FRET systems, such as metal-organic frameworks.

## 4. Experimental Section

*Methods*: One-photon excited fluorescence spectra measurements were performed at room temperature and a CW HeCd laser emitting at 325 nm and a Xenon lamp were used as the excitation source. The emission of the samples was collected from the edge and the signals were dispersed by a 750 mm monochromator combined with suitable filters, and detected by a photomultiplier tube (Hamamatsu R928) using a standard lock-in amplifier technique. Excitation spectra were obtained using a 450 W Xenon lamp monochromated with a double Czerny-Turner spectrometer (GEMINI 180) whose intensity was pre-corrected. TRPL spectra were carried out at room temperature by using TCSPC technique, with a resolution of 10 ps (PicoQuant PicoHarp 300). The second harmonic generation of Titanium sapphire laser (Chameleon, Coherent Inc.) operating at 360 nm (100 fs, 80 MHz) was used as the excitation source. TPA cross-sections of linear and tetrahedral molecules were measured using Z-scan technique.[15,16] These compounds were dissolved in THF and filled in 1 mm quartz cells, with a concentration of $1 \times 10^{-3}$ M. The samples were excited with femtosecond pulses from the Mai-Tai laser (80 MHz, 100 fs, Spectra-Physics, Inc.), with tunable wavelength range from 720 to 920 nm. In the measurements, the input laser beam was first passed through a beam chopper with an open ratio of 50/50 and a rotating speed of 315 rounds per second. Then the Gaussian beam was tightly focused into the samples by a convex lens (f = 10 cm). The radius of focal spot size was 35 μm, needed for obtaining peak intensity. The pumping pulse energy inside the samples was changed from 0.04 to 0.4 μJ using an adjustable attenuator. The transmitted beam was detected by a silicon photodiode using the standard lock-in amplifier technique. The experimental setup for the measurements of two-photon excited fluorescence spectra was the same as that used in the case of one-photon excitation, while the excitation source was the same as that used in Z-scan measurements. Two-photon excited fluorescence images were taken by an objective (50×, numerical aperture = 0.42) and delivered to a camera. A low-pass filter (<720 nm) was used to block excitation light. For the measurements of three to five-photon emission spectra, the laser pulses from an OPA combined with TOPAS (1000 Hz, 110 fs, Spectra-Physics, Inc.) with tunable wavelength range from 900 to 2.6 μm were used as excitation source. The experiments were performed in THF solutions with a concentration of $5 \times 10^{-4}$ M (for three- and four-photon absorption) or $1 \times 10^{-3}$ M (for five-photon absorption), respectively, filled in 10 mm thick cells. The input pulse energy range from 0.3 to 20 μJ was used in the measurements. For the photobleaching tests on one-photon emission from the close-packed films, an unfocused 325 nm laser beam,

with a beam radius of 1 mm and pumping power of 16 mW, was used. When testing the photostability of samples under two-photon excitation, a slightly focused laser beam (beam radius = 2.5 mm, pulse energy = 0.01 or 0.1 μJ) was utilized.

## Supporting Information

Supporting Information is available from the Wiley Online Library or from the author.

## Acknowledgements

[1] a) G. S. He, H. S. Oh, P. N. Prasad, *Opt. Lett.* **2011**, *36*, 4431; b) T. C. He, W. Wei, L. Ma, R. Chen, S. Wu, H. Zhang, Y. Yang, J. Ma, L. Huang, G. G. Gurzadyan, H. D. Sun, *Small* **2012**, *8*, 2163.

[2] a) S. Hotta, T. Yamao, *J. Mater. Chem.* **2011**, *21*, 1295; b) H. Fang, S. Lu, X. Zhan, J. Feng, Q. Chen, H. Wang, X. Liu, H. Sun, *Org. Electron.* **2013**, *14*, 762.

[3] T. C. He, R. Chen, W. W. Lin, F. Huang, H. D. Sun, *Appl. Phys. Lett.* **2011**, *99*, 081902.

[4] N. G. Horton, K. Wang, D. Kobat, C. Clark, F. Wise, C. Schaffer, C. Xu, *Nat. Photonics* **2013**, *7*, 205.

[5] G. S. He, L. S. Tan, Q. Zheng, P. N. Prasad, *Chem. Rev.* **2008**, *108*, 1245.

[6] T. C. He, Z. B. Lim, L. Ma, H. Li, D. Rajwar, Y. Ying, Z. Di, A. C. Girmsdale, H. D. Sun, *Chem. Asian J.* **2013**, *8*, 564.

[7] D. Ding, K. Li, W. Qin, R. Zhan, Y. Hu, J. Liu, B. Z. Tang, B. Liu, *Adv. Healthcare Mater.* **2013**, *2*, 500.

[8] S. B. Noh, R. H. Kim, W. J. Kim, S. Kim, K. Lee, N. S. Cho, H. Shim, H. E. Pudavar, P. N. Prasad, *J. Mater. Chem.* **2010**, *20*, 7422.

[9] a) N. Tian, Q.-H. Xu, *Adv. Mater.* **2007**, *19*, 1988; b) D. W. Brousmiche, J. M. Serin, J. M. J. Fréchet, G. S. He, T. Lin, S. J. Chung, P. N. Prasad, *J. Am. Chem. Soc.* **2003**, *125*, 1448; c) G. D. Scholes, G. R. Fleming, A. Olaya-Castro, R. V. Grondelle, *Nat. Chem.* **2011**, *3*, 763.

[10] K. E. Sapsford, L. Berti, I. L. Medintz, *Angew. Chem. Int. Ed.* **2006**, *45*, 4562.

[11] F. He, X. S. Ren, X. Q. Shen, Q.-H. Xu, *Macromolecules* **2011**, *44*, 5373.

[12] C. Wang, T. Zhang, W. Lin, *Chem. Rev.* **2012**, *112*, 1084.

[13] C. Y. Lee, O. K. Farha, B. J. Hong, A. A. Sarjeant, S. T. Nguyen, J. T. Hupp, *J. Am. Chem. Soc.* **2011**, *133*, 15858.

[14] X. Zhang, M. A. Ballem, Z. Hu, P. Bergman, K. Uvdal, *Angew. Chem. Int. Ed.* **2011**, *50*, 5729.

[15] H. Son, S. Jin, S. Patwardhan, S. J. Wezenberg, N. C. Jeong, M. So, C. E. Wilmer, A. A. Sarjeant, G. C. Schatz, R. Q. Snurr, O. K. Farha, G. P. Wiederrecht, J. T. Hupp, *J. Am. Chem. Soc.* **2013**, *135*, 862.

[16] T. C. He, D. Rajwar, L. Ma, Y. Wang, Z. B. Lim, A. C. Grimsdale, H. D. Sun, *Appl. Phys. Lett.* **2012**, *101*, 213302.

[17] Z. B. Lim, H. Li, S. Sun, J. Y. Lek, A. Trewin, Y. M. Lam, A. C. Grimsdale, *J. Mater. Chem.* **2012**, *22*, 6218.

[18] M. Sheik-Bahae, A. A. Said, E. W. Van Stryland, *Opt. Lett.* **1989**, *14*, 955.

[19] M. Sheik-Bahae, A. A. Said, T. H. Wei, D. J. Haga, E. W. Van Stryland, *IEEE J. Quantum Electron.* **1990**, *26*, 760.

[20] S. Chung, K. Kim, T. Lin, G. S. He, J. Swiatkiewicz, P. N. Prasad, *J. Phys. Chem. B* **1999**, *103*, 10741.

[21] a) L. Guo, K. F. Li, M. S. Wong, K. W. Cheah, *Chem. Commun.* **2013**, *49*, 3597; b) H. H. Fan, K. F. Li, X. L. Zhang, W. Yang, M. S. Wong, K. W. Cheah, *Chem. Commun.* **2011**, *47*, 3879; c) Z. L. Huang, N. Li, H. Lei, Z. R. Qiu, H. Z. Wang, Z. P. Zhong, Z. H. Zhou, *Chem. Commun.* **2002**, 2400.

[22] a) S. Kwak, S. Yang, N. R. Kim, J. H. Kim, B. Bae, *Adv. Mater.* **2011**, *23*, 5767; b) A. Wild, A. Teichler, C. Ho, X. Wang, H. Zhan, F. Schlutter, A. Winter, M. D. Hager, W. Wong, U. S. Schubert, *J. Mater. Chem. C* **2013**, *1*, 1812.

[23] R. Chen, V. D. Ta, F. Xiao, Q. Zhang, H. D. Sun, *Small* **2013**, *9*, 1052.

[24] P. T. K. Chin, R. A. M. Hikmet, S. C. J. Meskers1, R. A. J. Janssen, *Adv. Funct. Mater.* **2007**, *17*, 3829.

[25] T. C. He, X. Qi, R. Chen, J. Wei, H. Zhang, H. D. Sun, *ChemPlusChem* **2012**, *77*, 688.

[26] F. Cucinotta, F. Carniato, A. Devaux, L. De Cola, L. Marchese, *Chem. Eur. J.* **2012**, *18*, 15310.

[27] G. Jiang, A. S. Susha, A. A. Lutich, F. D. Stefani, J. Feldmann, A. L. Rogach, *ACS Nano* **2009**, *3*, 4127.

[28] A. G. Harpur, F. S. Wouters, P. I. H. Bastiaens, *Nat. Biotechnol.* **2001**, *19*, 167.

[29] A. A. Lutich, G. Jiang, A. S. Susha, A. L. Rogach, F. D. Stefani, J. Feldmann, *Nano Lett.* **2009**, *9*, 2636.

[30] a) S. Jin, H.-J. Son, O. K. Farha, G. Wiederrecht, J. T. Hupp, *J. Am. Chem. Soc.* **2013**, *135*, 955; b) Z. Xu, C. R. Hine, M. M. Maye, Q. Meng, M. Cotlet, *ACS Nano* **2012**, *6*, 4984.

[31] M. H. Stewart, A. L. Huston, A. M. Scott, A. L. Efros, J. S. Melinger, K. B. Gemmill, S. A. Trammell, J. B. Blanco-Canosa, P. E. Dawson, I. L. Medintz, *ACS Nano* **2012**, *6*, 5330.

[32] S. Ramachandra1, Z. D. Popovic, K. C. Schuermann, F. Cucinotta, G. Calzaferri, L. D. Cola, *Small* **2011**, *7*, 1488.

[33] a) J. Luo, Z. Xie, J. W. Y. Lam, L. Cheng, H. Chen, C. Qiu, H. S. Kwok, X. Zhan, Y. Liu, D. Zhu, B. Z. Tang, *Chem. Commun.* **2001**, 1740; b) B. Gao, H. Wang, Y. Hao, L. Fu, H. Fang, Y. Jiang, L. Wang, Q. Chen, H. Xia, L. Pan, Y. Ma, H. Sun, *J. Phys. Chem. B* **2010**, *114*, 128.

[34] a) M. Cotlet, T. Vosch, S. Habuchi, T. Weil, K. Müllen, J. Hofkens, F. D. Schryver, *J. Am. Chem. Soc.* **2005**, *127*, 9760; b) D. Liu, S. D. Feyter, M. Cotlet, A. Stefan, U. Wiesler, A. Herrmann, D. Grebel-Koehler, J. Qu, K. Müllen, F. C. D. Schryver, *Macromolecules* **2003**, *36*, 5918; c) E. G. Moore, P. V. Bernhardt, A. Pigliucci, M. J. Riley, E. Vauthey, *J. Phys. Chem. A* **2003**, *107*, 8396.

[35] M. Drobizhev, A. Karotki, M. Kruk, A. Rebane, *Chem. Phys. Lett.* **2002**, *355*, 175.

[36] F. Wang, X. Liu, *Chem. Soc. Rev.* **2009**, *38*, 976.

[37] Z. Deutsch, L. Neeman, D. Oron, *Nat. Nanotechnol.* **2013**, DOI: 10.1038/nnano.2013.146.

[38] L. Cerdán, E. Enciso, V. Martín, J. Bañuelos, I. López-Arbeloa, A. Costela, I. García-Moreno, *Nat. Photonics* **2012**, *6*, 621.